Ginsenoside Rg1 promotes β-amyloid peptide degradation through inhibition of the ERK/PPARγ phosphorylation pathway in an Alzheimer's disease neuronal model

QIANKUN QUAN[1], XINXIN MA[2], MING LI[1], XI LI[1] and HAIFENG YUAN[3]

Departments of [1]Geriatrics, [2]Psychology and [3]Rehabilitation, The Second Affiliated
Hospital of Xi'an Jiaotong University, Xi'an, Shaanxi 710004, P.R. China

Abstract. β-Amyloid peptide (Aβ) deposition in the brain is an important pathological change in Alzheimer's disease (AD). Insulin-degrading enzyme (IDE), which is regulated transcriptionally by peroxisome proliferator-activated receptor γ (PPARγ), is able to proteolyze Aβ. One of the members of the MAPK family, ERK, is able to mediate the phosphorylation of PPARγ at Ser112, thereby inhibiting its transcriptional activity. Ginsenoside Rg1 is one of the active ingredients in the natural medicine ginseng and has inhibitory effects on Aβ production. The present study was designed to investigate whether ginsenoside Rg1 is able to affect the regulation of PPARγ based on the expression of its target gene, *IDE*, and whether it is able to promote Aβ degradation via inhibition of the ERK/PPARγ phosphorylation pathway. In the present study, primary cultured rat hippocampal neurons were treated with $A\beta_{1\text{-}42}$, ginsenoside Rg1 and the ERK inhibitor PD98059, and subsequently TUNEL staining was used to detect the level of neuronal apoptosis. ELISA was subsequently employed to detect the intra- and extracellular $A\beta_{1\text{-}42}$ levels, immunofluorescence staining and western blotting were used to detect the translocation of ERK from the cytoplasm to the nucleus, immunofluorescence double staining was used to detect the co-expression of ERK and PPARγ, and finally, western blotting was used to detect the phosphorylation of PPARγ at Ser112 and IDE expression. The results demonstrated that ginsenoside Rg1 or PD98059 were able to inhibit primary cultured hippocampal neuron apoptosis induced by $A\beta_{1\text{-}42}$ treatment, reduce the levels of intra- and extraneuronal $A\beta_{1\text{-}42}$ and inhibit the translocation of ERK from the cytoplasm to the nucleus. Furthermore, administration of ginsenoside Rg1 or PD98059 resulted in attenuated co-expression of ERK and PPARγ, inhibition of phosphorylation of PPARγ at Ser112 mediated by ERK and an increase in IDE expression. In addition, the effects when PD98059 to inhibit ERK followed by treatment with ginsenoside Rg1 were found to be more pronounced than those when using PD98059 alone. In conclusion, ginsenoside Rg1 was demonstrated to exert neuroprotective effects on AD via inhibition of the ERK/PPARγ phosphorylation pathway, which led to an increase in IDE expression, the promotion of Aβ degradation and the decrease of neuronal apoptosis. These results could provide a theoretical basis for the clinical application of ginsenoside Rg1 in AD.

Introduction

β-Amyloid peptide (Aβ) deposition in the brain is one of the most important pathological changes that occur in Alzheimer's disease (AD) (1). Previous studies have suggested that Aβ is able to cause the phosphorylation of the tubulin associated unit protein, which leads to the formation of neurofibrillary tangles (2), in addition to exerting a role in synaptic dysfunction (3), neuron loss (4), microglia activation and neuroinflammation (5), calcium deregulation (6), oxidative stress (7), mitochondrial dysfunction (8), and cholinergic dysfunction (9), all of which ultimately affect cognitive function and lead to the development of AD. Insulin-degrading enzyme (*IDE*) is a target gene of a nuclear transcription factor called peroxisome proliferator-activated receptor (PPAR) γ (10). IDE is able to effectively proteolyze Aβ in the brain (11). At present, targeted IDE therapy has become one of the hotspots of research for AD treatment (12).

Ginseng is the dried root of *Panax ginseng*, which has been used as a natural medicine for thousands of years in Asia, especially in China, due its effects of reinforcing vitality, increasing bodily resistance and enhancing cognitive ability (13,14). Ginsenoside Rg1 is one of the active ingredients of ginseng, and it has been demonstrated to exert numerous neuroprotective effects on AD (15), including alleviating oxidative stress damage (16), improving the bioenergetics and morphology of mitochondria (17), and

Correspondence to: Professor Haifeng Yuan, Department of Rehabilitation, The Second Affiliated Hospital of Xi'an Jiaotong University, 157 Xiwu Road, Xi'an, Shaanxi 710004, P.R. China
E-mail: 2422561017@qq.com

altering the gut microbiota (18). A recent study (19) indicated that ginsenoside Rg1 exerts a scavenging effect on Aβ, which is able to inhibit the phosphorylation of PPARγ at Ser273 through inhibition of the cyclin-dependent kinase 5 expression pathway, subsequently reducing Aβ production and exerting neuroprotective effects on AD by affecting the expression levels of *IDE* and β-amyloid cleavage enzyme 1 (*BACE1*), which are targeted by PPARγ. The MAPK family comprises a series of serine-threonine protein kinases that form a common signaling pathway through which extracellular signals elicit nuclear responses such as gene expression, cell proliferation and apoptosis (20,21). Upon activation by extracellular stimulation, MAPK is translocated from the cytoplasm to the nucleus, thereby causing the phosphorylation of nuclear transcription factors, and subsequently regulates the transcriptional levels of the corresponding genes (22). It has been demonstrated that ERK, a member of the MAPK family, is able to mediate the phosphorylation of the A/B structural domain of PPARγ at Ser112, thereby inhibiting its transcriptional activity (23).

The present study aimed to investigate whether ginsenoside Rg1 could affect the regulation of PPARγ based on the expression of its target gene, *IDE*, and whether it could promote Aβ degradation via inhibition of the ERK/PPARγ phosphorylation pathway.

Materials and methods

Reagents. Ginsenoside Rg1 was purchased from Baoji Chenguang Biotechnology Co., Ltd.; it has the molecular formula $C_{42}H_{72}O_{14}$, a molecular weight of 801.01 and high-performance liquid chromatography was performed by Baoji Chenguang Biotechnology Co., Ltd. to determine that the purity was ~98%. Dulbecco's modified Eagle's medium, neurobasal medium and B27 were purchased from Gibco; Thermo Fisher Scientific, Inc., fetal bovine serum was purchased from Biological Industries, glutamine and cytarabine were purchased from Aladdin, goat serum was purchased from Beijing Solarbio, $Aβ_{1-42}$ was purchased from MilliporeSigma and PD98059 was purchased from Abcam. Streptomycin, penicillin and rabbit anti-rat phosphorylated (p-)PPARγ-Ser112 (cat. no. LM-3737R) polyclonal antibody were obtained from LMAI Bio Co., Ltd. Mouse anti-rat ERK monoclonal antibody (cat. no. bsm-33232M), and rabbit anti-rat ERK (cat. no. bs-0022R), IDE (cat. no. bs-0018R), PPARγ (cat. no. bs-4590R), Histone H3 (cat. no. bs-17422R), GAPDH (cat. no. bs-41373R) and β-actin (cat. no. bs-0061R) polyclonal antibodies were purchased from BIOSS. Horseradish peroxidase-labeled goat anti-rabbit secondary antibody (cat. no. WLA023), and the TUNEL assay, BCA protein concentration assay (cat. no. WLA004), whole cell lysis assay (cat. no. WLA019) and nuclear and cytoplasmic protein extraction (cat. no. WLA020) kits, and ECL luminescent solution were purchased from Wanleibio Co., Ltd. $Aβ_{1-42}$ ELISA kit (cat. no. CEA946Ra) was purchased from Wuhan USCN Business Co., Ltd. Trypsin, RIPA, DAPI, Cy3-labeled goat anti-rabbit IgG (cat. no. A0516; for red fluorescence) and FITC-labeled goat anti-mouse IgG (cat. no. A0568; for green fluorescence) were obtained from Beyotime Institute of Biotechnology.

Rat hippocampal neuron isolation and culture. A total of 130 2-day-old Sprague-Dawley rats (weight range, 8-10 g; males, 65; females, 65) were purchased from the Experimental Animal Center of Xi'an Jiaotong University Health Science Center [License no. SCXK (Shaan) 2018-001]. These animals were kept in a specific pathogen-free facility with a 12/12-h light/dark cycle at a temperature of 25˚C and a humidity of 50-65% and were allowed free access to breastmilk from their mothers before the study began. After being obtained, these animals were temporarily housed in a cage covered with soft bedding at a temperature of 25˚C, and then moved to a specialized room where euthanasia via decapitation was performed. Before euthanasia, the health and behavior of these animals, including their mental and breathing state, and activity, and whether these animals exhibited anxiety, restlessness and squeaking, were monitored every 15 min. To minimize suffering and distress, the animals were rapidly decapitated using a clean, sharp and regularly maintained guillotine device (cat. no. ZK-ZSQ-SD; ChiCo JX Co., Ltd.) by a skilled operator, and then, the brain tissue was removed under aseptic conditions. Subsequently, the hippocampal tissue was isolated, digested with trypsin and centrifuged (310 x g; 7 min; 25˚C) to obtain the neurons. The neurons were inoculated into six-well culture plates at a density of $5x10^5$ cells/ml and incubated with Dulbecco's modified Eagle's medium containing 10% fetal bovine serum at 37˚C in an atmosphere of 5% CO_2 and saturated humidity for 8 h. Then, Dulbecco's modified Eagle's medium was changed to neurobasal medium containing glutamine (0.5 mmol/l), B27 (2%), streptomycin (100 U/ml) and penicillin (100 U/ml) at 37˚C for 48 h. Subsequently, cytarabine (10 μM) was added to inhibit glial cell growth. The solution was changed every 3 days. The rat hippocampal neurons, which were observed to be maturing and forming networks after ~15 days of incubation at 37˚C, were ready for subsequent experiments.

Drug administration. Drug administration was performed at 25˚C and repeated 6 times. The cultured neurons were divided into a blank control group, a model group and a ginsenoside Rg1 treatment group. The neurons of the model group were treated with $Aβ_{1-42}$ (final concentration, 8 μM) (24) for 24 h, whereas the neurons of the ginsenoside Rg1 group was pretreated with ginsenoside Rg1 (final concentration, 60 μM) (25) for 1 h and subsequently co-treated with $Aβ_{1-42}$ (final concentration, 8 μM) for 24 h; by contrast, no drugs were administered to the neurons of the blank control group. To further confirm that ginsenoside Rg1 exerts anti-Aβ effects through acting on ERK to regulate PPARγ phosphorylation, the ERK inhibitor PD98059 was used to inhibit ERK, and the effects of ginsenoside Rg1 on $Aβ_{1-42}$-treated neurons were observed. The neurons were divided into three groups as follows: i) Model group, cultured neurons were treated with $Aβ_{1-42}$ (final concentration, 8 μM) for 24 h; ii) PD98059 group, the cultured neurons were pretreated with PD98059 (final concentration, 20 μM) (26) for 1 h, and subsequently co-treated with $Aβ_{1-42}$ (final concentration, 8 μM) for 24 h; and iii) ginsenoside Rg1 + PD98059 group, the cultured neurons were treated with PD98059 (final concentration, 20 μM) for 0.5 h, subsequently ginsenoside Rg1 (final concentration, 60 μM) was added for pretreatment for 1 h, and finally, $Aβ_{1-42}$ (final concentration, 8 μM) was added for co-treatment for 24 h.

TUNEL staining. After cultured cells were placed on the poly-L-lysine-coated slides (cell density, 70-80%), they were dried at 25˚C. Subsequently, cells were immersed in 4% paraformaldehyde solution and fixed for 30 min at 25˚C. Next, 0.1% Triton X-100/10 mM PBS was added dropwise to permeabilize the cells for 5 min. After rinsing with PBS, the TUNEL reaction solution was added dropwise to the cells, and the mixture was incubated for 60 min at 37˚C with humidification away from light. Subsequently, cells were rinsed with PBS, followed by counterstaining with DAPI (5.7 μM) in the dark for 5 min at 25˚C. After having been rinsed with PBS again, the slides were sealed with a fluorescence quencher. Neurons were counted by two pathologists under a fluorescence microscope (cat. no. BX53; Olympus Corporation) at a magnification of x400 in a blinded manner. Each pathologist observed four random fields of view of each slide. First, the total numbers of neurons (DAPI+ neurons) and apoptotic neurons (TUNEL+ neurons) in each field of view were determined to obtain the percentage of apoptotic neurons. Then, the average percentage of apoptotic neurons was evaluated for the four fields of view using the results from each pathologist. Finally, the average percentage from the two pathologists was calculated as the final result.

Immunofluorescence staining. After fixing the neurons with 4% paraformaldehyde for 15 min at 25˚C, 0.1% Triton X-100 was added for permeabilization for 30 min at 25˚C. 10% goat serum was subsequently added dropwise for blocking for 15 min at 25˚C. The rabbit anti-rat ERK antibody (1:200) was then added for a 12 h incubation at 4˚C. After washing with PBS, Cy3-labeled goat anti-rabbit IgG (for red fluorescence; 1:200) was added, with a further incubation for 60 min at 25˚C away from the light. Subsequently, the nuclei were subjected to counterstaining with DAPI in the dark for 5 min at 25˚C. Finally, slides were sealed by dropwise addition of fluorescence quencher. ERK subcellular localization in the neurons was observed under a fluorescence microscope (BX53; Olympus Corporation).

To observe the binding of ERK to PPARγ, immunofluorescence double staining was performed for ERK and PPARγ. The neurons were fixed with 4% paraformaldehyde for 15 min at 25˚C, and then permeabilized with 0.1% Triton X-100 for 30 min at 25˚C. After blocking the neurons with 10% goat serum for 15 min at 25˚C, rabbit anti-rat polyclonal PPARγ antibody (1:200) and mouse anti-rat ERK monoclonal antibody (1:200) were added for incubation overnight at 4˚C. After washing with PBS, Cy3-labeled goat anti-rabbit IgG (for red fluorescence; 1:200) and FITC-labeled goat anti-mouse IgG (for green fluorescence; 1:200) were added for incubation for 60 min at 25˚C in the dark. After rinsing with PBS, the nuclei were counterstained with DAPI in the dark for 5 min at 25˚C. After rinsing a further time with PBS, the fluorescence quencher was added dropwise to mount the slides. Finally, the sites of expression of ERK and PPARγ in the neurons were observed under a fluorescence microscope (cat. no. BX53; Olympus Corporation).

ELISA. The cultured cells were collected and lysed on ice for 15 min by adding a lysis solution of RIPA and PMSF (ratio, 100:1). Subsequently, the cells were centrifuged at 12,000 x g for 10 min at 4˚C. After separating the supernatant from the pellet, the level of intracellular Aβ was detected using a rat $A\beta_{1-42}$ ELISA kit (Wuhan USCN Business Co., Ltd.) according to the manufacturer's instructions. To detect the level of extracellular $A\beta_{1-42}$, the culture medium of each group was collected and centrifuged at 3,000 x g for 10 min at 4˚C to obtain the supernatant. The concentration of $A\beta_{1-42}$ in the supernatant was detected using the aforementioned rat $A\beta_{1-42}$ ELISA kit according to the manufacturer's instructions.

Western blotting. The neuronal nuclear protein, cytoplasmic protein and total protein fractions were extracted respectively using nuclear and cytoplasmic protein extraction and whole cell lysis assay kits (Wanleibio Co., Ltd.) according to the instructions of these kits. A BCA assay was performed to determine protein concentration (Wanleibio Science Co., Ltd.). Subsequently, the proteins were denatured by heating at 95˚C, and 40 μg protein was loaded each electrophoretic lane and separated by electrophoresis on 8% SDS-PAGE gels. After having been transferred to nitrocellulose membranes, the separated proteins were subjected to blocking using 5% skimmed milk powder at 37˚C for 1 h. Subsequently, the levels of nuclear and cytoplasmic ERK protein, nuclear PPARγ, nuclear p-PPARγ-Ser112 protein and whole-cell IDE protein were separately measured. Nitrocellulose membranes were incubated with rabbit anti-rat ERK, p-PPARγ-Ser112, PPARγ, IDE, Histone H3, GAPDH and β-actin polyclonal antibodies (diluted in 5% skimmed milk powder; 1:600, 1:500, 1:500, 1:800, 1:800, 1:800 and 1:1,000, respectively), overnight at 4˚C, followed by washes with Tris-buffered saline containing 0.05% Tween 20. Subsequently, nitrocellulose membranes were treated with horseradish peroxidase-labeled goat anti-rabbit secondary antibody (1:900) at 37˚C for 45 min. Protein bands were visualized using an ECL chemiluminescent reagent. Gel-Pro-Analyzer software (version 4.0; Media Cybernetics, Inc.) was used to analyze the optical density values of the target bands, with Histone H3 as the loading control for nuclear ERK, p-PPARγ-Ser112 and PPARγ proteins, with GAPDH on cytoplasmic ERK protein and with β-actin on whole IDE protein.

Statistical analysis. Data are presented as the mean ± SEM obtained from 6 independent experiments. Statistical analyses were performed using SPSS (version 19.0; IBM Corp.). One-way ANOVA was used for comparisons among groups, followed by the least significant difference post hoc test for pairwise comparisons between groups. $P<0.05$ was considered to indicate a statistically significant difference.

Results

Neuroprotective effects of ginsenoside Rg1 on an AD neuronal model. After treating primary cultured hippocampal neurons with $A\beta_{1-42}$, number of TUNEL+ neurons, as detected by TUNEL staining, was increased significantly (control group vs. model group; $P<0.05$), which suggested that $A\beta_{1-42}$ could induce neuronal apoptosis. Pretreatment with ginsenoside Rg1 prior to treatment with $A\beta_{1-42}$ was found to reduce the TUNEL+ rate in neurons (ginsenoside Rg1 group vs. model group; $P<0.05$), indicating that ginsenoside Rg1 could effectively reduce neuronal apoptosis in the AD model (Fig. 1A and B).
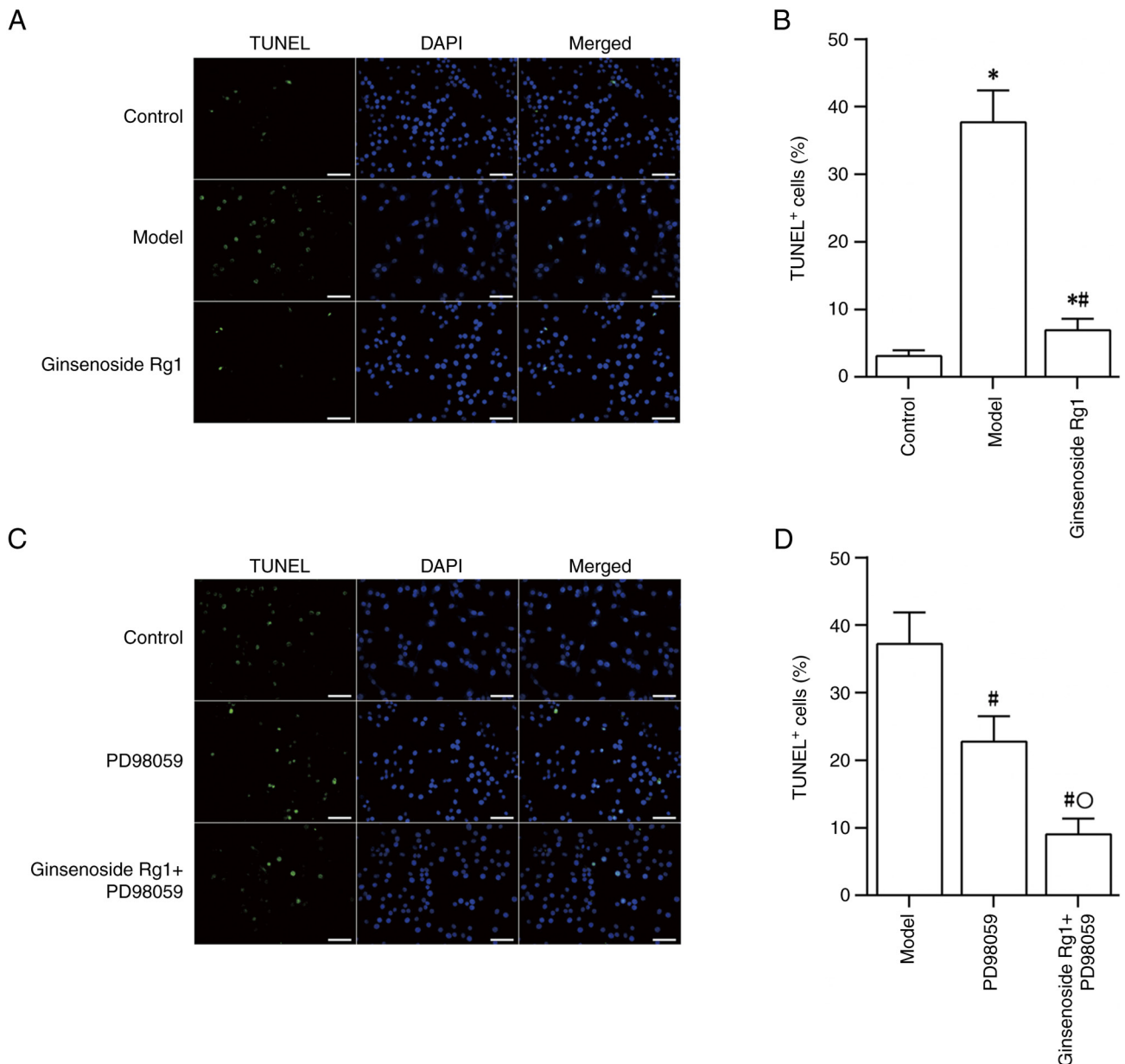
Figure 1. Effect of ginsenoside Rg1 on neuronal apoptosis in an Alzheimer's disease model. (A) TUNEL staining. (B) Comparison of numbers of TUNEL+ neurons. (C) TUNEL staining following ERK inhibition. (D) Comparison of the numbers of TUNEL+ neurons following ERK inhibition. Green represents TUNEL+ staining in the nucleus, whereas blue represents DAPI-stained nuclei (scale bar, 50 μm; n=6). *P<0.05 vs. control group, #P<0.05 vs. model group and °P<0.05 vs. PD98059 group.

The use of the ERK inhibitor PD98059 also led to a reduction in the rate of neuronal apoptosis induced by $A\beta_{1-42}$ (model group vs. PD98059 group; P<0.05). Treatment with PD98059 followed by ginsenoside Rg1 resulted in a further decrease in neuronal apoptosis compared with that resulting from treatment with PD98059 alone (PD98059 group vs. ginsenoside Rg1 + PD98059; P<0.05; Fig. 1C and D).

Ginsenoside Rg1 reduces the level of Aβ in an AD neuronal model. ELISA results demonstrated that treatment of primary cultured rat hippocampal neurons with $A\beta_{1-42}$ could lead to significantly increased intra- and extracellular levels of $A\beta_{1-42}$ (control group vs. model group; P<0.05). However, treatment with ginsenoside Rg1 reduced the intra- and extracellular $A\beta_{1-42}$ levels in the AD neuronal model (model group vs.

ginsenoside Rg1 group; P<0.05; Fig. 2A and B). Treatment with PD98059 also reduced the intra- and extracellular levels of $A\beta_{1-42}$ in the AD neuronal model (model group vs. PD98059 group; P<0.05; Fig. 2C and D). Following ERK inhibition by PD98059 in the AD neuronal model, treatment with ginsenoside Rg1 resulted in a further decrease in the intra- and extracellular $A\beta_{1-42}$ levels compared with the levels detected following treatment with PD98059 alone (PD98059 group vs. ginsenoside Rg1 + PD98059 group; P<0.05; Fig. 2C and D).

Ginsenoside Rg1 prevents ERK translocation from the cytoplasm to the nucleus in an AD neuronal model. To examine the effect of Aβ and ginsenoside Rg1 on ERK translocation, ERK expression and its subcellular localization in neurons were first observed using immunofluorescence staining.
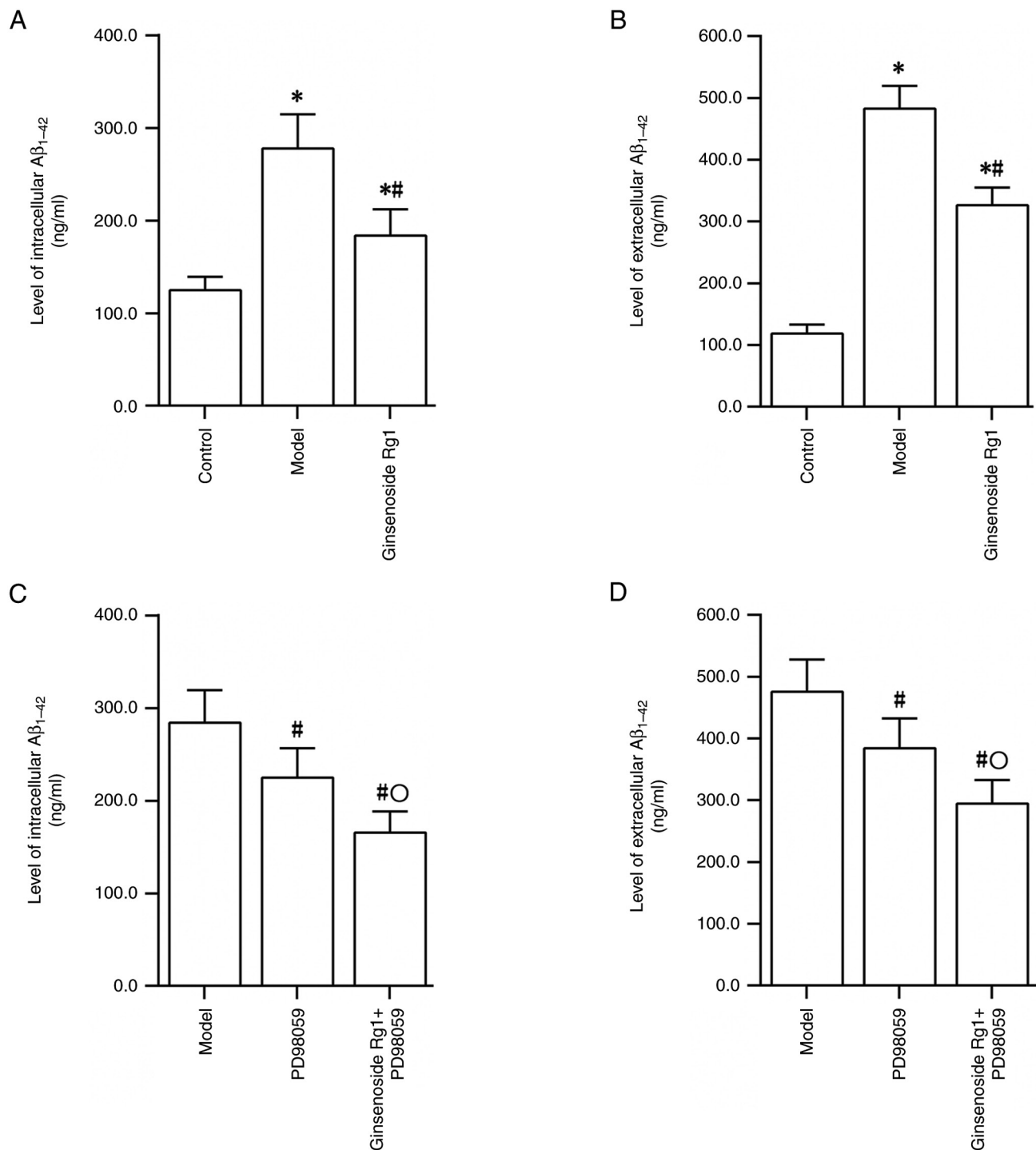
Figure 2. Effect of ginsenoside Rg1 on the Aβ levels in the neurons of an Alzheimer's disease model. (A) Comparisons of intracellular Aβ levels. (B) Comparisons of extracellular Aβ levels. (C) Comparisons of intracellular Aβ levels after ERK inhibition. (D) Comparisons of extracellular Aβ levels after ERK inhibition. Detection of intra- and extra-neuronal Aβ levels using ELISA (n=6). *P<0.05 vs. control group, $^{#}$P<0.05 vs. model group and $^{\circ}$P<0.05 vs. PD98059 group. Aβ, β-Amyloid peptide.

The results revealed that, when compared with the intensity of red fluorescent staining in normal neurons, the ERK red fluorescent staining in the cytoplasm of neurons treated with Aβ$_{1-42}$ was diminished, whereas that in the nucleus was enhanced. Compared with that in the Aβ$_{1-42}$-treated neurons (model group), pretreatment with ginsenoside Rg1 prior to Aβ$_{1-42}$ treatment resulted in enhanced ERK red fluorescence in the cytoplasm and reduced red fluorescence in the nuclei of the neurons (Fig. 3A). To further examine the translocation of ERK, the expression levels of the ERK protein in the cytoplasm and the nucleus were also detected using western blotting, and the ratio of the ERK protein expression in the nucleus relative to that in the cytoplasm was calculated. These results indicated that compared with those in the control group, ERK protein expression in the cytoplasm of neurons was decreased, whereas that in the nucleus was increased in the model group (all P<0.05); therefore, the ratio of ERK protein expression in the nucleus to that in the cytoplasm was
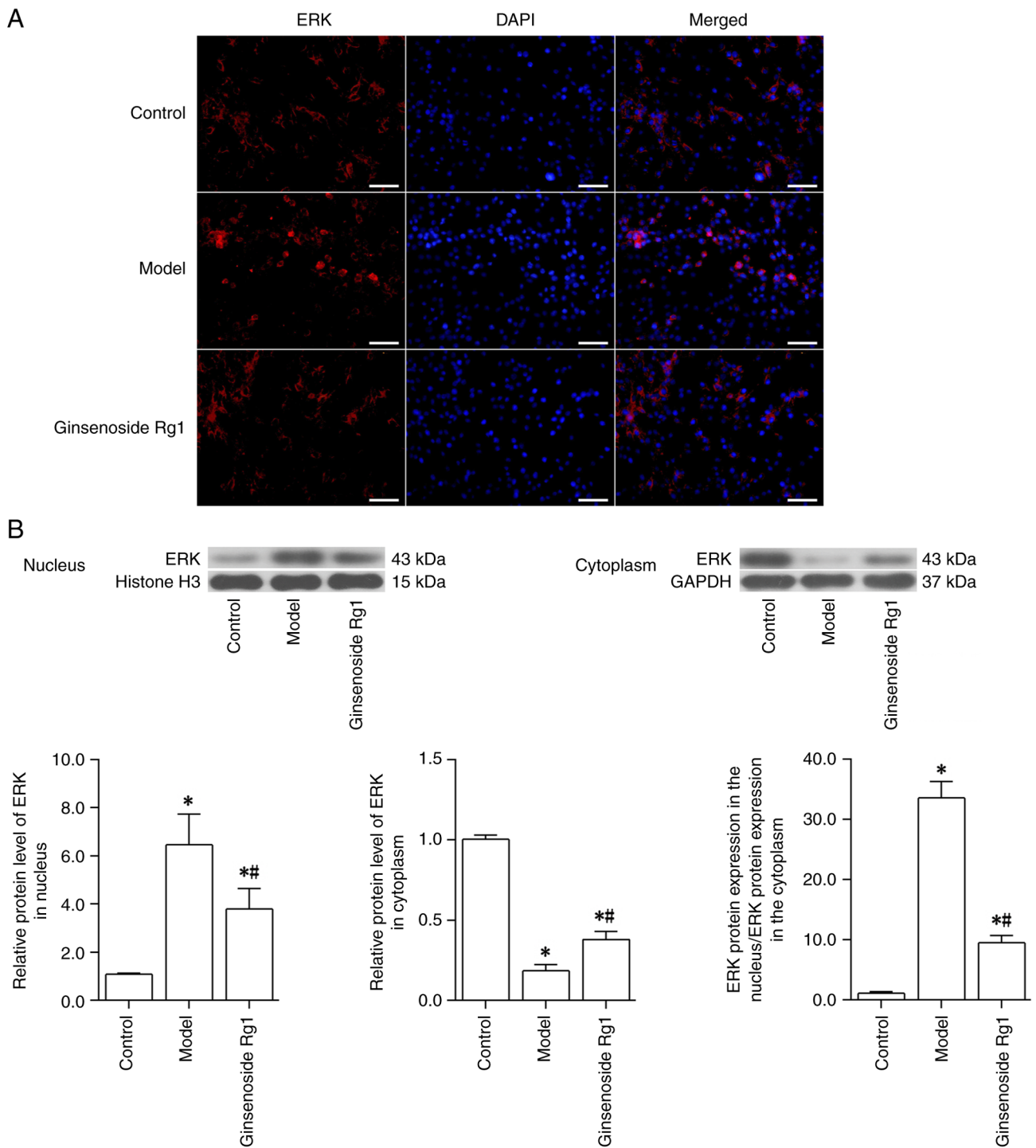
Figure 3. Effect of ginsenoside Rg1 on ERK translocation in the neurons of an Alzheimer's disease model. (A) ERK immunofluorescence staining. Red represents ERK staining, whereas blue represents DAPI-stained nuclei (scale bar, 50 μm). (B) Western blotting was used to detect the nuclear and cytoplasmic protein expression levels of ERK. Comparisons of the nuclear and cytoplasmic protein expression levels of ERK, and the ratio of ERK protein expression in the nucleus to that in the cytoplasm (n=6). *P<0.05 vs. control group and #P<0.05 vs. model group.

increased following $A\beta_{1-42}$ treatment (control group vs. model group; P<0.05). However, pretreatment with ginsenoside Rg1 effectively inhibited the $A\beta_{1-42}$-induced changes in ERK expression in the cytoplasm and in the nucleus; ERK protein expression in the cytoplasm was increased, whereas that in the nucleus was decreased, indicating that the ratio of ERK protein expression in the nucleus to that in the cytoplasm was decreased (model group vs. ginsenoside Rg1 group; all P<0.05;

Fig. 3B). Taken together, these results suggested that $A\beta_{1-42}$ could promote the translocation of ERK from the cytoplasm to the nucleus, whereas ginsenoside Rg1 was able to inhibit this translocation of ERK.

Ginsenoside Rg1 inhibits the co-expression of ERK and PPARγ in an AD neuronal model. To further confirm the binding of ERK to its target molecule, PPARγ, following
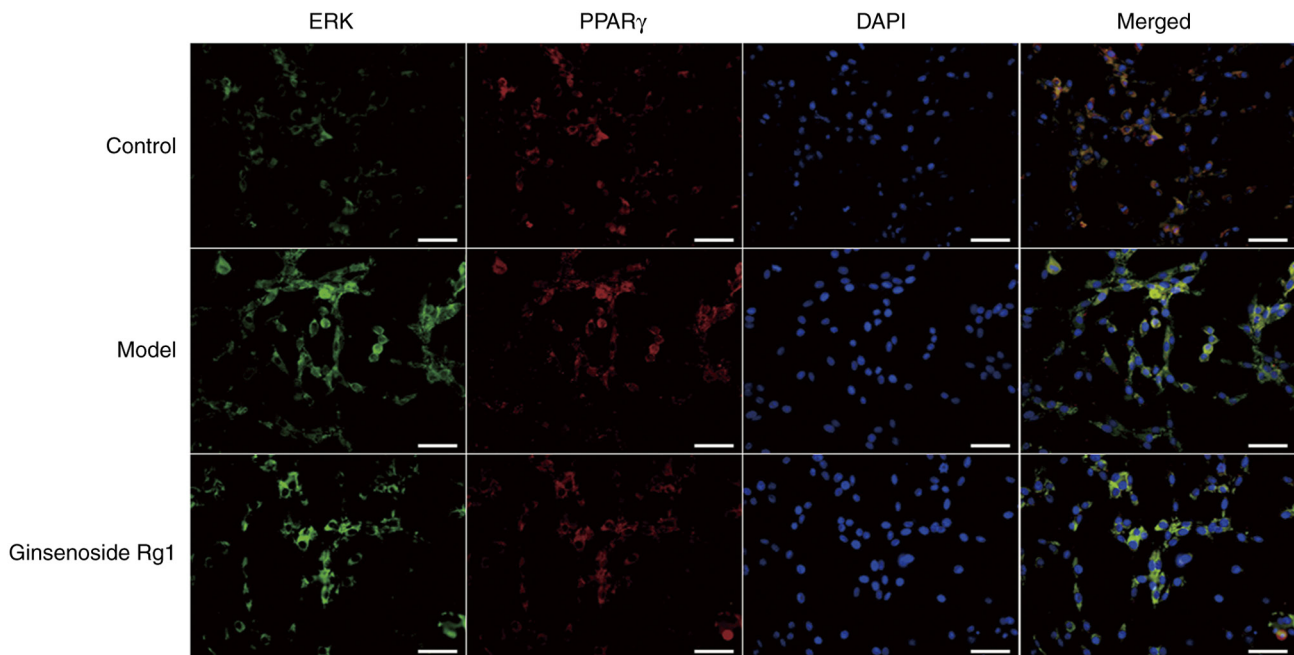
Figure 4. Effect of ginsenoside Rg1 on the co-expression of ERK and PPARγ in the neurons of an Alzheimer's disease model. Green represents ERK staining, red represents PPARγ staining and blue represents DAPI-stained nuclei (scale bar, 50 μm). PPARγ, peroxisome proliferator-activated receptor γ.

translocation from the cytoplasm to the nucleus, immunofluorescence double staining of ERK and PPARγ was performed to detect their co-expression levels. The co-expression of ERK and PPARγ in the nuclei of $A\beta_{1-42}$-treated hippocampal neurons was increased compared with that in the nuclei of normal neurons (model group vs. control), whereas the co-expression of ERK and PPARγ was lower in the nuclei of neurons that were pretreated with ginsenoside Rg1 prior to $A\beta_{1-42}$ treatment compared with that in the nuclei of neurons treated with $A\beta_{1-42}$ alone (ginsenoside Rg1 group vs. model group). These findings suggested that ginsenoside Rg1 could inhibit the co-expression of ERK and PPARγ in the AD neuronal model (Fig. 4).

Ginsenoside Rg1 inhibits the phosphorylation of PPARγ at Ser112 in an AD neuronal model. The phosphorylation level of PPARγ at Ser112 (p-PPARγ-Ser112/PPARγ) in the nucleus of the AD neuronal model following $A\beta_{1-42}$ and ginsenoside Rg1 treatment was investigated. The results revealed that the level of p-PPARγ-Ser112 was increased after treatment of primary cultured hippocampal neurons with $A\beta_{1-42}$ (control group vs. model group; $P<0.05$; Fig. 5A). However, pretreatment with ginsenoside Rg1 prior to treatment with $A\beta_{1-42}$ reduced the level of p-PPARγ at Ser112 (model group vs. ginsenoside Rg1 group; $P<0.05$; Fig. 5A). Following treatment with the ERK inhibitor PD98059 in the AD neuronal model, it was found that the level of p-PPARγ at Ser112 was reduced (model group vs. PD98059 group; $P<0.05$; Fig. 5B). Following ERK inhibition by PD98059 and treatment with ginsenoside Rg1 in the AD neuronal model, the level of p-PPARγ at Ser112 was not further decreased compared with that of the group treated with PD98059 alone (PD98059 group vs. ginsenoside Rg1 + PD98059; $P>0.05$; Fig. 5B). Taken together, these findings suggested that PD98059 and ginsenoside Rg1 were able to effectively inhibit the phosphorylation of PPARγ at Ser112 in the nuclei of the AD neuronal model.

Ginsenoside Rg1 increases IDE protein expression in an AD neuronal model. In a subsequent series of experiments, the effect of ginsenoside Rg1 on IDE protein expression in the AD neuronal model was examined using western blotting. The results demonstrated that IDE protein expression in the AD neuronal model, prepared by treating hippocampal neurons with $A\beta_{1-42}$, was decreased (control group vs. model group; $P<0.05$; Fig. 6A). However, IDE protein expression in the AD neuronal model was increased following treatment with ginsenoside Rg1 (model group vs. ginsenoside Rg1 group; $P<0.05$; Fig. 6A). IDE protein expression in the AD neuronal model was increased following treatment with PD98059 (model group vs. PD98059 group; $P<0.05$; Fig. 6B). However, IDE protein expression was increased further following pretreatment with PD98059 combined with treatment with ginsenoside Rg1 in the AD neuronal model (PD98059 group vs. ginsenoside Rg1 + PD98059 group; $P<0.05$; Fig. 6B).

Discussion

The findings presented in the current study further demonstrated the scavenging effect of ginsenoside Rg1 on Aβ, and the results suggested that the underlying mechanism might be associated with the inhibition of the ERK-mediated phosphorylation of PPARγ. Ginsenoside Rg1 prevents ERK translocation from the cytoplasm to the nucleus in an Alzheimer's disease neuronal model, resulting in the inhibition of PPARγ phosphorylation at Ser112 and the promotion of the transcriptional activity of PPARγ. As a result, the target gene of PPARγ *IDE* expression increases to promote Aβ degradation (Fig. 7). ERK regulates numerous downstream transcription factors, such as PPARγ (27), NF-κB (28), E-twenty-six-like transcription factor 1 (29), c-Myc (30) and c-Fos (31). Some molecules, such as BACE1 (32,33) and IDE (10,11), can be regulated
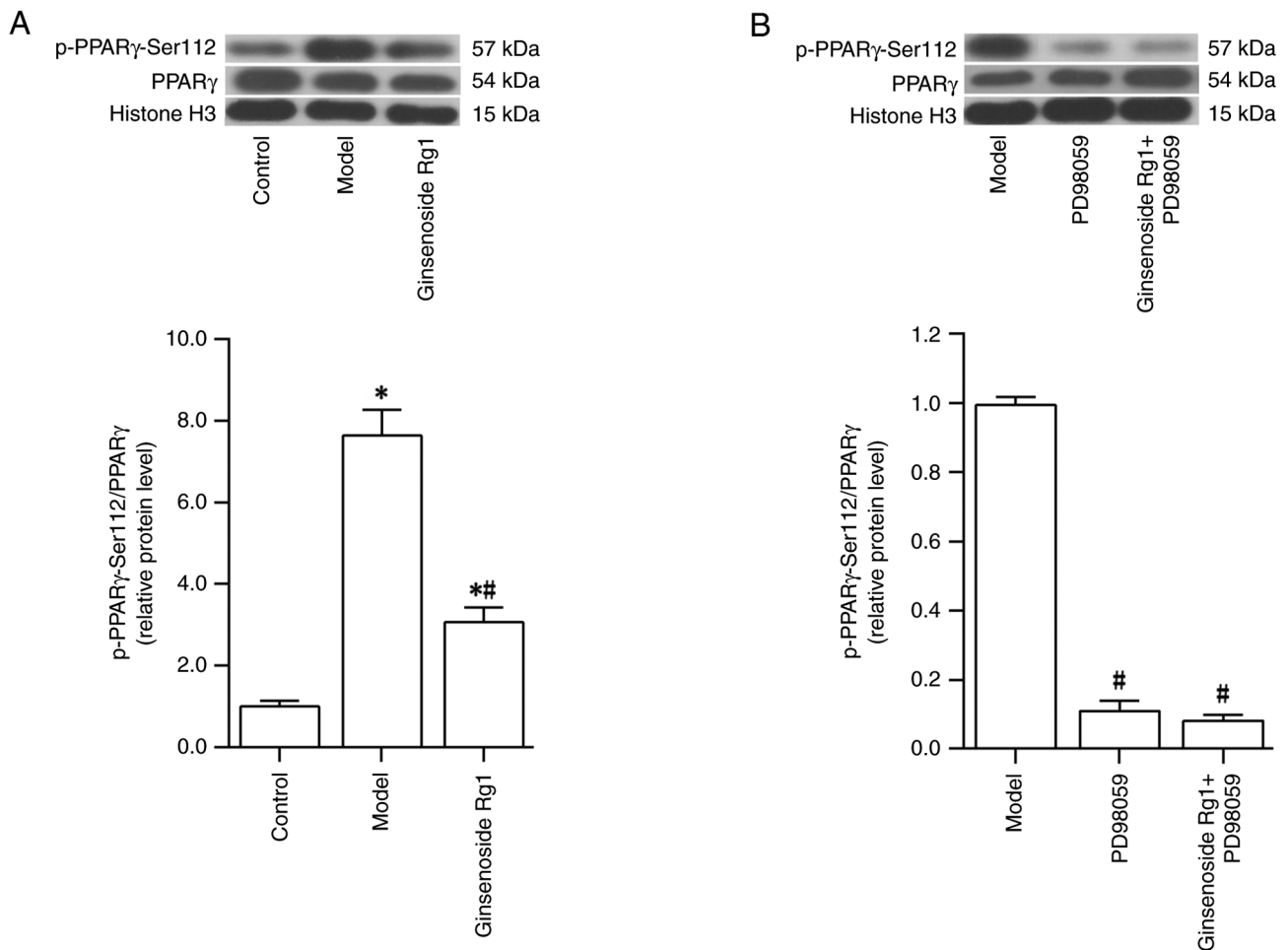
Figure 5. Effect of ginsenoside Rg1 on the phosphorylation of PPARγ at Ser112 in the nuclei of neurons of an Alzheimer's disease model. (A) Comparison of the phosphorylation levels of PPARγ at Ser112 (p-PPARγ-Ser112/PPARγ) in the nuclei of neurons. (B) Comparison of the phosphorylation levels of PPARγ at Ser112 (p-PPARγ-Ser112/PPARγ) in the nuclei of neurons following ERK inhibition (n=6). *$P<0.05$ vs. control group and #$P<0.05$ vs. model group. p-, phosphorylated; PPARγ, peroxisome proliferator-activated receptor γ.

transcriptionally by PPARγ, and are involved in the pathogenesis of AD. Therefore, PPARγ was chosen as the subject of the present study. PPARγ is a ligand-activated nuclear transcription factor that binds to retinoic X receptors to form heterodimers, subsequently binding to its ligand, and thereby regulating the expression of downstream target genes that are involved in the regulation of numerous physiological responses, including those associated with lipid metabolism, cell fate, glucose homeostasis, insulin sensitivity, immune responses and inflammation (34-36). Previous studies have also demonstrated that PPARγ is not only associated with obesity, diabetes, inflammation and tumors, but is also closely associated with AD (37,38). Furthermore, a previous study (39) demonstrated that PPARγ activation improved spatial memory in animal models of AD, and it was accomplished by inhibiting β-secretase expression and reducing Aβ production through modulating the responses of the microglia to Aβ deposition, thereby increasing the phagocytosis of Aβ and reducing cytokine release (40,41). Furthermore, it also accomplished this by improving mitochondrial function in AD models (42), reducing oxidative stress (43) and improving impaired synaptic plasticity (44).

The functions of PPARγ are regulated by post-translational modifications, including ubiquitination, phosphorylation, acetylation, SUMOylation and O-GlcNAcylation (45). As aging progresses, PPARγ phosphorylation inactivation occurs in various tissues, such as the kidney, cerebral cortex and adipose tissue (46). Bartl *et al* (47) showed that PPARγ phosphorylation is also present in the brains of patients with AD, and the number of p-PPARγ+ cells was found to be notably increased in the cortex and hippocampus of deceased patients with AD compared with those in age-matched control patients without dementia. In addition, a previously published *in vitro* study confirmed that the presence of Aβ can result in the phosphorylation of PPARγ at Ser273 (19). However, in the present study, Aβ treatment of the primary cultured rat hippocampal neurons resulted in an increase in the level of PPARγ phosphorylation at Ser112. At present, no definitive answer may be provided as to whether PPARγ phosphorylation leads to the onset of AD, or whether PPARγ phosphorylation occurs after the onset of AD.

Previous studies have demonstrated that certain stimuli such as epidermal growth factor, transforming growth factor β, insulin and prostaglandin F2α can trigger PPARγ phosphorylation at different sites through the activation of
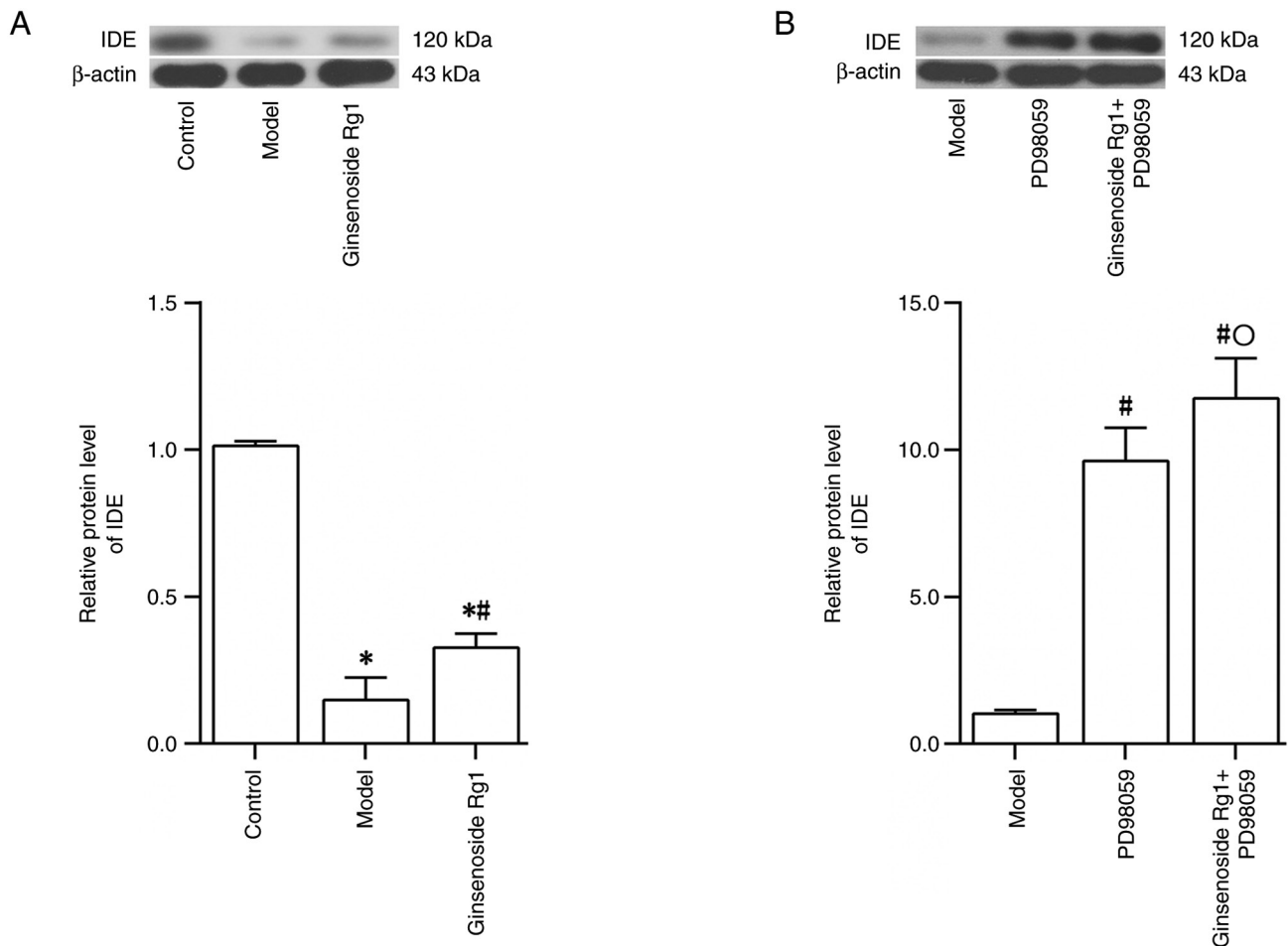
Figure 6. Effect of ginsenoside Rg1 on the IDE expression in the neurons of an Alzheimer's disease model. (A) Comparison of IDE protein expression in the neurons. (B) Comparison of IDE protein expression in the neurons after ERK inhibition (n=6). *P<0.05 vs. control group, $^#$P<0.05 vs. model group and $^○$P<0.05 vs. PD98059 group. IDE, insulin-degrading enzyme.
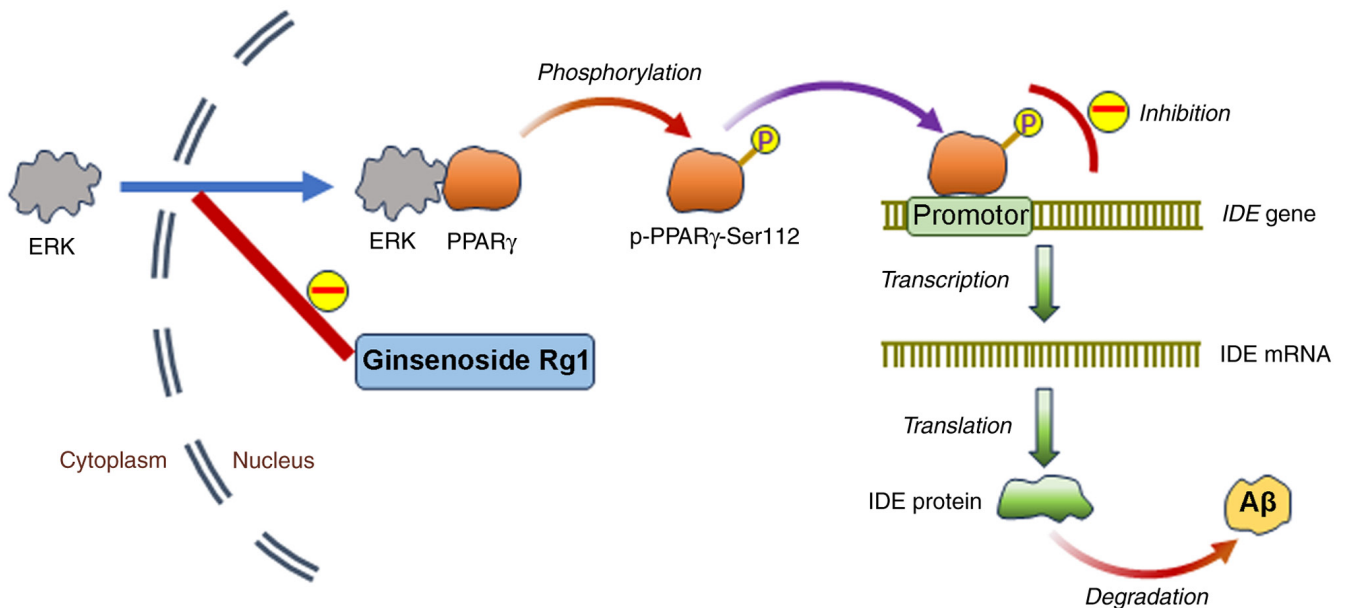

Figure 7. Possible mechanisms via which ginsenoside Rg1 promotes Aβ degradation by inhibiting the ERK/PPARγ phosphorylation pathway. IDE, which can be regulated transcriptionally by PPARγ, is able to proteolyze Aβ. After translocation from the cytoplasm to the nucleus, ERK can mediate the phosphorylation of PPARγ at Ser112, thereby inhibiting its transcriptional activity. The present study showed that ginsenoside Rg1 prevents ERK translocation from the cytoplasm to the nucleus in an Alzheimer's disease neuronal model, consequently resulting in the inhibition of PPARγ phosphorylation at Ser112 and the increase of IDE expression and promoting Aβ degradation. Aβ, β-Amyloid peptide; PPARγ, peroxisome proliferator-activated receptor γ; IDE, insulin-degrading enzyme; p-, phosphorylated.

MAPK, thereby leading to the increase or decrease of transcriptional activity of PPARγ (45,48,49). MAPK comprises a family of serine/threonine protein kinases, which are able to transmit numerous extracellular signals to the nucleus to regulate various cellular processes, including cell proliferation, gene expression, apoptosis, differentiation and stress responses (20,21). The MAPK signaling pathway includes three main kinases, including MAPK, MAPK kinase (MAPKK) and MAPKK kinase (MAPKKK). Stimuli, such as growth factor receptors, receptor tyrosine kinase and G-protein-coupled receptors, are able to activate Ras, which in turn activates MAPKKK. Activated MAPKKK subsequently phosphorylates and activates MAPKK which phosphorylates and activates MAPK (50). Following activation, MAPK is translocated from the cytoplasm into the nucleus where it binds to its target molecules via docking-mediated interactions, followed by serine/threonine-residue phosphorylation of multiple substrate proteins and the modification of their activity (22). The main members of the MAPK family are ERKs, p38 and JNK. It has been demonstrated that ERK and p38 mediate the Ser112 phosphorylation of the A/B structural domain of PPARγ, thereby inhibiting its transcriptional activity (23,27,51). In addition, JNK can mediate the phosphorylation of PPARγ at Ser82, also inhibiting its transcriptional activity (52). IDE is a zinc metalloprotease and is regulated transcriptionally by PPARγ (10). Previous studies have demonstrated that, in addition to its ability to degrade insulin, IDE is also able to effectively degrade Aβ, including intra- and extracellular Aβ (53,54). In the present study, the following observations were made after treating primary cultured rat hippocampal neurons with Aβ: ERK was translocated from the cytoplasm to the nucleus, the phosphorylation level of PPARγ at Ser112 was increased, IDE expression was decreased and neuronal apoptosis was increased. These findings suggested that Aβ could stimulate ERK translocation to the nucleus, thereby mediating the phosphorylation of PPARγ, and consequently affecting the PPARγ-mediated regulation of IDE expression. In the present study, treatment with ginsenoside Rg1 effectively inhibited the translocation of ERK from the cytoplasm to the nucleus and inhibited the co-expression of ERK and PPARγ. It was also found that the phosphorylation of PPARγ at Ser112 was reduced, IDE expression was increased, and both intra- and extracellular levels of Aβ were reduced, suggesting that ginsenoside Rg1 might exert an anti-Aβ effect by inhibiting the ERK-mediated phosphorylation of PPARγ. However, the present study did have certain limitations. First, the mechanisms through which Aβ affects the translocation of ERK from the cytoplasm to the nucleus, how ginsenoside Rg1 inhibits ERK or whether the MAPK signaling pathway is involved in this process have not been revealed. In addition to its inhibitory effect on PPARγ via the phosphorylation of Ser112, ERK can also induce nuclear export of PPARγ via direct interactions with PPARγ, thereby modulating the nucleo-cytoplasmic compartmentalization of PPARγ and attenuating the transactivation function of PPARγ (55). It is also unclear whether Aβ promotes the aforementioned ERK-mediated nuclear export of PPARγ, or whether ginsenoside Rg1 may inhibit the ERK-mediated nuclear export of PPARγ. Relevant experiments will be performed in the future to address these questions.

PPARγ belongs to a family of ligand-regulated nuclear receptors with other members including PPARα, PPARβ and PPARδ (56). Previous studies have demonstrated that PPARα, PPARβ, PPARδ are also associated with AD (56-60). PPARα is able to regulate the expression of genes encoding enzymes that are engaged in amyloid precursor protein metabolism and downregulate BACE1 expression to reduce Aβ generation (56). By contrast, PPARβ and PPARδ can alleviate AD through their insulin-sensitizing, anti-inflammatory and myelin sheath-stabilizing effects, thereby decreasing Aβ deposition (57). It has been demonstrated that PPARδ activation may exert a neuroprotective effect in AD models by inhibiting the inflammation and the amelioration of $Aβ_{1-42}$-induced hippocampal neurotoxicity (58,59). Additionally, PPARδ has been demonstrated to suppress the generation of neurotoxic Aβ by attenuating BACE1 expression via the cytokine signaling 1-mediated inhibition of signal transducer and activator of transcription 1 signaling (60). In the present study, only the effects of ginsenoside Rg1 on PPARγ were observed. Therefore, it is not yet clear whether ginsenoside Rg1 also exerts any effects on PPARα, PPARβ, PPARδ.

The present study revealed that ERK pathway activation could induce cellular apoptosis, and that the inhibitor PD98059 inhibited cell apoptosis, findings that were consistent with those of numerous previous studies (61-63). The ERK pathway not only mediates cell proliferation but can also induce apoptosis (64). Activation of the ERK signaling pathway is able to promote the proliferation of tumor cells and enhance the processes of tumor cell migration and invasion (65-68), all of which leads to an acceleration of tumor progression. PD98059 could exert a positive protective effect, as it can inhibit tumor cell proliferation, migration and invasion (66,69-71). In addition, activation of the ERK pathway has been demonstrated to mediate cell apoptosis, and this effect can be blocked by PD98059 (61-63). In cardiomyocytes, ERK activation is involved in doxorubicin-induced cardiomyocyte apoptosis, which has been demonstrated to be blocked by the knockdown of ERK (61). In rats with pre-eclampsia, activation of the ERK signaling pathway has been demonstrated to induce trophoblast apoptosis (62). Furthermore, in IL-1β-stimulated chondrocytes, ERK has been demonstrated to be involved in the dynamin-related protein 1-mediated induction of apoptosis, and apoptosis can be inhibited by PD98059 (63). However, it appears that several studies have obtained contrary findings. For example, in colorectal cancer cells, treatment with PD98059 combined with paclitaxel led to an increase in apoptosis (72). Another study showed that activation of ERK improve the cell viability of H_2O_2-treated bone marrow-derived mesenchymal stem cells, and the effect could be blocked by PD98059 and ERK small interfering RNA (73). Therefore, further studies are required to fully clarify whether the effects of ERK activation and PD98059 on apoptosis are inhibitory or stimulatory, and these studies will be performed in the future.

In the present study, use of the ERK inhibitor PD98059, followed by treatment with ginsenoside Rg1, was found to result in significant improvements in Aβ levels, neuronal apoptosis and IDE expression in an AD neuronal model compared with the effects of PD98059 treatment alone. This suggested that, in addition to the ERK/PPARγ pathway,

ginsenoside Rg1 might also increase the levels and activity of IDE and promote Aβ degradation through other pathways. Besides PPARγ, IDE levels have been shown to be regulated by other molecules and signaling factors/processes, including circulating insulin, glucose, L-lactate and free fatty acids (74), nucleoside triphosphates (75), sex steroids (76) and insulin-mediated Akt activation (77). However, further studies are required to confirm whether ginsenoside Rg1 may affect IDE expression through these pathways or act on IDE directly. In addition to IDE, certain other proteases are known to degrade Aβ, including neprilysin, MMP-9 and MMP-2 (78). In other studies, it has been shown that ginsenoside Rg1 is able to i) decrease accumulation of neurofibrillary tangles in the retina by regulating the activities of neprilysin and protein kinase A in the retinal cells of an AD mouse model (79); ii) inhibit tumor cell invasion and migration by inhibiting NF-κB-dependent MMP-9 expression (80); and iii) inhibit myocardial remodeling in an animal model of chronic thromboembolic pulmonary hypertension through upregulating MMP-2 and MMP-9 expression in myocardial tissue (81). However, to the best of our knowledge, whether ginsenoside Rg1 removes Aβ by acting on these molecules is unknown, and further studies are required to investigate this possibility.

There are two further limitations of the present study. First, only immunofluorescence double staining was used to detect the combination of ERK and PPARγ in the AD neuronal model used in the present study. It would have been useful to investigate the effect of Aβ and ginsenoside Rg1 on the combination of ERK and PPARγ using co-immunoprecipitation. In addition, only *in vitro* experiments were performed in the present study and, although this does not substantially affect conclusions, the results of the present study would be more impactful, and the conclusion would be strengthened if animal experiments had been conducted.

In conclusion, the present study demonstrated that ginsenoside Rg1 may exert neuroprotective effects on AD by inhibiting the ERK/PPARγ phosphorylation pathway, which thereby upregulated the expression levels of the PPARγ-targeted gene *IDE* and promoted Aβ degradation. These findings have presented evidence in favor of a novel mechanism of action of ginsenoside Rg1 against AD, also providing a theoretical basis for a further application of ginsenoside Rg1 in the treatment of AD.

Availability of data and materials

The datasets used and/or analyzed during the current study are available from the corresponding author on reasonable request.

Authors' contributions

HY, QQ and XL designed the study. QQ and HY wrote the manuscript. QQ, XM and ML performed the experiments. HY, QQ and XM collected and analyzed the data. HY and QQ confirm the authenticity of all the raw data. All authors read and approved the final version of the manuscript.

Ethics approval and consent to participate

All experimental procedures in the present study were approved by The Ethics Committee of Xi'an Jiaotong University Health Science Center (approval no. 2020-942; Xi'an, China).

Patient consent for publication

Not applicable.

Competing interests

The authors declare that they have no competing interests.

References

1. Murphy MP and LeVine H III: Alzheimer's disease and the amyloid-beta peptide. J Alzheimers Dis 19: 311-323, 2010.
2. Seino Y, Kawarabayashi T, Wakasaya Y, Watanabe M, Takamura A, Yamamoto-Watanabe Y, Kurata T, Abe K, Ikeda M, Westaway D, *et al*: Amyloid β accelerates phosphorylation of tau and neurofibrillary tangle formation in an amyloid precursor protein and tau double-transgenic mouse model. J Neurosci Res 88: 3547-3554, 2010.
3. Chen Y, Fu AKY and Ip NY: Synaptic dysfunction in Alzheimer's disease: Mechanisms and therapeutic strategies. Pharmacol Ther 195: 186-198, 2019.
4. Jawhar S, Trawicka A, Jenneckens C, Bayer TA and Wirths O: Motor deficits, neuron loss, and reduced anxiety coinciding with axonal degeneration and intraneuronal Aβ aggregation in the 5XFAD mouse model of Alzheimer's disease. Neurobiol Aging 33: 196.e29-e40, 2012.
5. Cai Z, Hussain MD and Yan LJ: Microglia, neuroinflammation, and beta-amyloid protein in Alzheimer's disease. Int J Neurosci 124: 307-321, 2014.
6. Esteras N and Abramov AY: Mitochondrial calcium deregulation in the mechanism of beta-amyloid and tau pathology. Cells 9: 2135, 2020.
7. Caruso G, Spampinato SF, Cardaci V, Caraci F, Sortino MA and Merlo S: β-amyloid and oxidative stress: Perspectives in drug development. Curr Pharm Des 25: 4771-4781, 2019.
8. Huang Z, Yan Q, Wang Y, Zou Q, Li J, Liu Z and Cai Z: Role of mitochondrial dysfunction in the pathology of amyloid-β. J Alzheimers Dis 78: 505-514, 2020.
9. Tran MH, Yamada K and Nabeshima T: Amyloid beta-peptide induces cholinergic dysfunction and cognitive deficits: A minireview. Peptides 23: 1271-1283, 2002.
10. Du J, Zhang L, Liu SB, Zhang C, Huang XQ, Li J, Zhao NM and Wang Z: PPARgamma transcriptionally regulates the expression of insulin-degrading enzyme in primary neurons. Biochem Biophys Res Commun 383: 485-490, 2009.
11. Sahoo BR, Panda PK, Liang W, Tang WJ, Ahuja R and Ramamoorthy A: Degradation of Alzheimer's amyloid-β by a catalytically inactive insulin-degrading enzyme. J Mol Biol 433: 166993, 2021.
12. Kurochkin IV, Guarnera E and Berezovsky IN: Insulin-degrading enzyme in the fight against Alzheimer's disease. Trends Pharmacol Sci 39: 49-58, 2018.
13. Hu BY, Liu XJ, Qiang R, Jiang ZL, Xu LH, Wang GH, Li X and Peng B: Treatment with ginseng total saponins improves the neurorestoration of rat after traumatic brain injury. J Ethnopharmacol 155: 1243-1255, 2014.
14. Bai L, Gao J, Wei F, Zhao J, Wang D and Wei J: Therapeutic potential of ginsenosides as an adjuvant treatment for diabetes. Front Pharmacol 9: 423, 2018.

15. Fang F, Chen X, Huang T, Lue LF, Luddy JS and Yan SS: Multi-faced neuroprotective effects of ginsenoside Rg1 in an Alzheimer mouse model. Biochim Biophys Acta 1822: 286-292, 2012.
16. Yang Y, Wang L, Zhang C, Guo Y, Li J, Wu C, Jiao J and Zheng H: Ginsenoside Rg1 improves Alzheimer's disease by regulating oxidative stress, apoptosis, and neuroinflammation through Wnt/GSK-3β/β-catenin signaling pathway. Chem Biol Drug Des 99: 884-896, 2022.
17. Kwan KKL, Yun H, Dong TTX and Tsim KWK: Ginsenosides attenuate bioenergetics and morphology of mitochondria in cultured PC12 cells under the insult of amyloid beta-peptide. J Ginseng Res 45: 473 481, 2021.
18. Wang L, Lu J, Zeng Y, Guo Y, Wu C, Zhao H, Zheng H and Jiao J: Improving Alzheimer's disease by altering gut microbiota in tree shrews with ginsenoside Rg1. FEMS Microbiol Lett 367: fnaa011, 2020.
19. Quan Q, Li X, Feng J, Hou J, Li M and Zhang B: Ginsenoside Rg1 reduces β-amyloid levels by inhibiting CDK5-induced PPARγ phosphorylation in a neuron model of Alzheimer's disease. Mol Med Rep 22: 3277-3288, 2020.
20. Urushibara N, Mitsuhashi S, Sasaki T, Kasai H, Yoshimizu M, Fujita H and Oda A: JNK and p38 MAPK are independently involved in tributyltin-mediated cell death in rainbow trout (Oncorhynchus mykiss) RTG-2 cells. Comp Biochem Physiol C Toxicol Pharmacol 149: 468-475, 2009.
21. Guo YJ, Pan WW, Liu SB, Shen ZF, Xu Y and Hu LL: ERK/MAPK signalling pathway and tumorigenesis. Exp Ther Med 19: 1997-2007, 2020.
22. Turjanski AG, Vaqué JP and Gutkind JS: MAP kinases and the control of nuclear events. Oncogene 26: 3240-3253, 2007.
23. Ge C, Cawthorn WP, Li Y, Zhao G, Macdougald OA and Franceschi RT: Reciprocal control of osteogenic and adipogenic differentiation by ERK/MAP kinase phosphorylation of Runx2 and PPARγ transcription factors. J Cell Physiol 231: 587-596, 2016.
24. Yang EJ, Ahn S, Ryu J, Choi MS, Choi S, Chong YH, Hyun JW, Chang MJ and Kim HS: Phloroglucinol attenuates the cognitive deficits of the 5XFAD mouse model of Alzheimer's disease. PLoS One 10: e0135686, 2015.
25. Li Y, Guan Y, Wang Y, Yu CL, Zhai FG and Guan LX: Neuroprotective effect of the ginsenoside Rg1 on cerebral ischemic injury in vivo and in vitro is mediated by PPARγ regulated antioxidative and anti-inflammatory pathways. Evid Based Complement Alternat Med 2017: 7842082, 2017.
26. Kiwanuka E, Junker JP and Eriksson E: Transforming growth factor β1 regulates the expression of CCN2 in human keratinocytes via Smad-ERK signalling. Int Wound J 14: 1006-1018, 2017.
27. El Ouarrat D, Isaac R, Lee YS, Oh DY, Wollam J, Lackey D, Riopel M, Bandyopadhyay G, Seo JB, Sampath-Kumar R and Olefsky JM: TAZ is a negative regulator of PPARγ activity in adipocytes and TAZ deletion improves insulin sensitivity and glucose tolerance. Cell Metab 31: 162-173.e5, 2020.
28. Jiang B, Xu S, Hou X, Pimentel DR, Brecher P and Cohen RA: Temporal control of NF-kappaB activation by ERK differentially regulates interleukin-1beta-induced gene expression. J Biol Chem 279: 1323-1329, 2004.
29. Mut M, Lule S, Demir O, Kurnaz IA and Vural I: Both mitogen-activated protein kinase (MAPK)/extracellular-signal-regulated kinases (ERK) 1/2 and phosphatidylinositide-3-OH kinase (PI3K)/Akt pathways regulate activation of E-twenty-six (ETS)-like transcription factor 1 (Elk-1) in U138 glioblastoma cells. Int J Biochem Cell Biol 44: 302-310, 2012.
30. Zuo Z, Liu J, Sun Z, Cheng YW, Ewing M, Bugge TH, Finkel T, Leppla SH and Liu S: ERK and c-Myc signaling in host-derived tumor endothelial cells is essential for solid tumor growth. Proc Natl Acad Sci USA 120: e2211927120, 2023.
31. Monje P, Hernández-Losa J, Lyons RJ, Castellone MD and Gutkind JS: Regulation of the transcriptional activity of c-Fos by ERK. A novel role for the prolyl isomerase PIN1. J Biol Chem 280: 35081-35084, 2005.
32. Lin N, Chen LM, Pan XD, Zhu YG, Zhang J, Shi YQ and Chen XC: Tripchlorolide attenuates β-amyloid generation via suppressing PPARγ-regulated BACE1 activity in N2a/APP695 cells. Mol Neurobiol 53: 6397-6406, 2016.
33. Sadleir KR, Eimer WA, Cole SL and Vassar R: Aβ reduction in BACE1 heterozygous null 5XFAD mice is associated with transgenic APP level. Mol Neurodegener 10: 1, 2015.
34. Wagner N and Wagner KD: The role of PPARs in disease. Cells 9: 2367, 2020.

35. Szanto A, Balint BL, Nagy ZS, Barta E, Dezso B, Pap A, Szeles L, Poliska S, Oros M, Evans RM, *et al*: STAT6 transcription factor is a facilitator of the nuclear receptor PPARγ-regulated gene expression in macrophages and dendritic cells. Immunity 33: 699-712, 2010.
36. Vallée A, Lecarpentier Y, Guillevin R and Vallée JN: Effects of cannabidiol interactions with Wnt/β-catenin pathway and PPARγ on oxidative stress and neuroinflammation in Alzheimer's disease. Acta Biochim Biophys Sin (Shanghai) 49: 853-866, 2017.
37. Janani C and Ranjitha Kumari BD: PPAR gamma gene-a review. Diabetes Metab Syndr 9: 46-50, 2015.
38. Prashantha Kumar BR, Kumar AP, Jose JA, Prabitha P, Yuvaraj S, Chipurupalli S, Jeyarani V, Manisha C, Banerjee S, Jeyabalan JB, *et al*: Minutes of PPAR-γ agonism and neuroprotection. Neurochem Int 140: 104814, 2020.
39. Rodriguez-Rivera J, Denner L and Dineley KT: Rosiglitazone reversal of Tg2576 cognitive deficits is independent of peripheral gluco-regulatory status. Behav Brain Res 216: 255-261, 2011.
40. Heneka MT, Sastre M, Dumitrescu-Ozimek L, Hanke A, Dewachter I, Kuiperi C, O'Banion K, Klockgether T, Van Leuven F and Landreth GE: Acute treatment with the PPARgamma agonist pioglitazone and ibuprofen reduces glial inflammation and Abeta1-42 levels in APPV717I transgenic mice. Brain 128: 1442-1453, 2005.
41. Yamanaka M, Ishikawa T, Griep A, Axt D, Kummer MP and Heneka MT: PPARγ/RXRα-induced and CD36-mediated microglial amyloid-β phagocytosis results in cognitive improvement in amyloid precursor protein/presenilin 1 mice. J Neurosci 32: 17321-17331, 2012.
42. Zolezzi JM, Silva-Alvarez C, Ordenes D, Godoy JA, Carvajal FJ, Santos MJ and Inestrosa NC: Peroxisome proliferator-activated receptor (PPAR) γ and PPARα agonists modulate mitochondrial fusion-fission dynamics: Relevance to reactive oxygen species (ROS)-related neurodegenerative disorders? PLoS One 8: e64019, 2013.
43. Nicolakakis N, Aboulkassim T, Ongali B, Lecrux C, Fernandes P, Rosa-Neto P, Tong XK and Hamel E: Complete rescue of cerebrovascular function in aged Alzheimer's disease transgenic mice by antioxidants and pioglitazone, a peroxisome proliferator-activated receptor gamma agonist. J Neurosci 28: 9287-9296, 2008.
44. Xu S, Liu G, Bao X, Wu J, Li S, Zheng B, Anwyl R and Wang Q: Rosiglitazone prevents amyloid-β oligomer-induced impairment of synapse formation and plasticity via increasing dendrite and spine mitochondrial number. J Alzheimers Dis 39: 239-251, 2014.
45. Brunmeir R and Xu F: Functional regulation of PPARs through post-translational modifications. Int J Mol Sci 19: 1738, 2018.
46. Ye P, Zhang XJ, Wang ZJ and Zhang C: Effect of aging on the expression of peroxisome proliferator-activated receptor gamma and the possible relation to insulin resistance. Gerontology 52: 69-75, 2006.
47. Bartl J, Monoranu CM, Wagner AK, Kolter J, Riederer P and Grünblatt E: Alzheimer's disease and type 2 diabetes: Two diseases, one common link? World J Biol Psychiatry 14: 233-240, 2013.
48. Hu E, Kim JB, Sarraf P and Spiegelman BM: Inhibition of adipogenesis through MAP kinase-mediated phosphorylation of PPARgamma. Science 274: 2100-2103, 1996.
49. Camp HS and Tafuri SR: Regulation of peroxisome proliferator-activated receptor gamma activity by mitogen-activated protein kinase. J Biol Chem 272: 10811-10816, 1997.
50. Irnaten M, Duff A, Clark A and O'Brien C: Intra-cellular calcium signaling pathways (PKC, RAS/RAF/MAPK, PI3K) in lamina cribrosa cells in glaucoma. J Clin Med 10: 62, 2020.
51. Stechschulte LA, Hinds TD Jr, Khuder SS, Shou W, Najjar SM and Sanchez ER: FKBP51 controls cellular adipogenesis through p38 kinase-mediated phosphorylation of GRα and PPARγ. Mol Endocrinol 28: 1265-1275, 2014.
52. Camp HS, Tafuri SR and Leff T: c-Jun N-terminal kinase phosphorylates peroxisome proliferator-activated receptor-gamma1 and negatively regulates its transcriptional activity. Endocrinology 140: 392-397, 1999.
53. Vingtdeux V, Chandakkar P, Zhao H, Blanc L, Ruiz S and Marambaud P: CALHM1 ion channel elicits amyloid-β clearance by insulin-degrading enzyme in cell lines and in vivo in the mouse brain. J Cell Sci 128: 2330-2338, 2015.
54. Quan Q, Qian Y, Li X and Li M: CDK5 participates in amyloid-β production by regulating PPARγ phosphorylation in primary rat hippocampal neurons. J Alzheimers Dis 71: 443-460, 2019.
55. Burgermeister E and Seger R: MAPK kinases as nucleo-cytoplasmic shuttles for PPARgamma. Cell Cycle 6: 1539-1548, 2007.

56. Wójtowicz S, Strosznajder AK, Jeżyna M and Strosznajder JB: The novel role of PPAR alpha in the brain: Promising target in therapy of Alzheimer's disease and other neurodegenerative disorders. Neurochem Res 45: 972-988, 2020.
57. Strosznajder AK, Wójtowicz S, Jeżyna MJ, Sun GY and Strosznajder JB: Recent insights on the role of PPAR-β/δ in neuroinflammation and neurodegeneration, and tts potential target for therapy. Neuromolecular Med 23: 86-98, 2021.
58. Malm T, Mariani M, Donovan LJ, Neilson L and Landreth GE: Activation of the nuclear receptor PPARδ is neuroprotective in a transgenic mouse model of Alzheimer's disease through inhibition of inflammation. J Neuroinflammation 12: 7, 2015.
59. An YQ, Zhang CT, Du Y, Zhang M, Tang SS, Hu M, Long Y, Sun HB and Hong H: PPARδ agonist GW0742 ameliorates Aβ1-42-induced hippocampal neurotoxicity in mice. Metab Brain Dis 31: 663-671, 2016.
60. Lee WJ, Ham SA, Lee GH, Choi MJ, Yoo H, Paek KS, Lim DS, Hong K, Hwang JS and Seo HG: Activation of peroxisome proliferator-activated receptor delta suppresses BACE1 expression by up-regulating SOCS1 in a JAK2/STAT1-dependent manner. J Neurochem 151: 370-385, 2019.
61. Zhang DX, Ma DY, Yao ZQ, Fu CY, Shi YX, Wang QL and Tang QQ: ERK1/2/p53 and NF-κB dependent-PUMA activation involves in doxorubicin-induced cardiomyocyte apoptosis. Eur Rev Med Pharmacol Sci 20: 2435-2442, 2016.
62. Song XP, Zhang YM, Sui SA, Li XY and Huang Y: Activation of the ERK1/2 signaling pathway enhances proliferation and apoptosis of trophoblast in preeclampsia rats. Eur Rev Med Pharmacol Sci 25: 598-604, 2021.
63. Ansari MY, Novak K and Haqqi TM: ERK1/2-mediated activation of DRP1 regulates mitochondrial dynamics and apoptosis in chondrocytes. Osteoarthritis Cartilage 30: 315-328, 2022.
64. Mebratu Y and Tesfaigzi Y: How ERK1/2 activation controls cell proliferation and cell death: Is subcellular localization the answer? Cell Cycle 8: 1168-1175, 2009.
65. Yan Z, Ohuchida K, Fei S, Zheng B, Guan W, Feng H, Kibe S, Ando Y, Koikawa K, Abe T, et al: Inhibition of ERK1/2 in cancer-associated pancreatic stellate cells suppresses cancer-stromal interaction and metastasis. J Exp Clin Cancer Res 38: 221, 2019.
66. Wang H, Du S, Cai J, Wang J and Shen X: Apolipoprotein E2 promotes the migration and invasion of pancreatic cancer cells via activation of the ERK1/2 signaling pathway. Cancer Manag Res 12: 13161-13171, 2020.
67. Chen S, Li Z, Wang Y and Fan S: BTN3A3 inhibits the proliferation, migration and invasion of ovarian cancer cells by regulating ERK1/2 phosphorylation. Front Oncol 12: 952425, 2022.
68. Xu H, Zhao H and Yu J: HOXB5 promotes retinoblastoma cell migration and invasion via ERK1/2 pathway-mediated MMPs production. Am J Transl Res 10: 1703-1712, 2018.
69. Wang G, Yin L, Peng Y, Gao Y, Gao H, Zhang J, Lv N, Miao Y and Lu Z: Insulin promotes invasion and migration of KRAS^{G12D} mutant HPNE cells by upregulating MMP-2 gelatinolytic activity via ERK- and PI3K-dependent signalling. Cell Prolif 52: e12575, 2019.
70. Xu Y, Gao F, Zhang J, Cai P and Xu D: Fibroblast growth factor receptor 2 promotes the proliferation, migration, and invasion of ectopic stromal cells via activation of extracellular-signal-regulated kinase signaling pathway in endometriosis. Bioengineered 13: 8360-8371, 2022.
71. Cheng XD, Gu JF, Yuan JR, Feng L and Jia XB: Suppression of A549 cell proliferation and metastasis by calycosin via inhibition of the PKC-α/ERK1/2 pathway: An in vitro investigation. Mol Med Rep 12: 7992-8002, 2015.
72. Li Y and Yang Q: Effect of PD98059 on chemotherapy in patients with colorectal cancer through ERK1/2 pathway. J BUON 24: 1837-1844, 2019.
73. Fang J, Zhao X, Li S, Xing X, Wang H, Lazarovici P and Zheng W: Protective mechanism of artemisinin on rat bone marrow-derived mesenchymal stem cells against apoptosis induced by hydrogen peroxide via activation of c-Raf-Erk1/2-p90^{rsk}-CREB pathway. Stem Cell Res Ther 10: 312, 2019.
74. González-Casimiro CM, Cámara-Torres P, Merino B, Diez-Hermano S, Postigo-Casado T, Leissring MA, Cózar-Castellano I and Perdomo G: Effects of fasting and feeding on transcriptional and posttranscriptional regulation of insulin-degrading enzyme in mice. Cells 10: 2466, 2021.
75. Camberos MC, Pérez AA, Udrisar DP, Wanderley MI and Cresto JC: ATP inhibits insulin-degrading enzyme activity. Exp Biol Med (Maywood) 226: 334-341, 2001.
76. George S, Petit GH, Gouras GK, Brundin P and Olsson R: Nonsteroidal selective androgen receptor modulators and selective estrogen receptor β agonists moderate cognitive deficits and amyloid-β levels in a mouse model of Alzheimer's disease. ACS Chem Neurosci 4: 1537-1548, 2013.
77. Zhao L, Teter B, Morihara T, Lim GP, Ambegaokar SS, Ubeda OJ, Frautschy SA and Cole GM: Insulin-degrading enzyme as a downstream target of insulin receptor signaling cascade: Implications for Alzheimer's disease intervention. J Neurosci 24: 11120-11126, 2004.
78. Humpel C: Organotypic vibrosections from whole brain adult Alzheimer mice (overexpressing amyloid-precursor-protein with the Swedish-Dutch-Iowa mutations) as a model to study clearance of beta-amyloid plaques. Front Aging Neurosci 7: 47, 2015.
79. He Y, Zhao H and Su G: Ginsenoside Rg1 decreases neurofibrillary tangles accumulation in retina by regulating activities of neprilysin and PKA in retinal cells of AD mice model. J Mol Neurosci 52: 101-106, 2014.
80. Li L, Wang Y, Qi B, Yuan D, Dong S, Guo D, Zhang C and Yu M: Suppression of PMA-induced tumor cell invasion and migration by ginsenoside Rg1 via the inhibition of NF-κB-dependent MMP-9 expression. Oncol Rep 32: 1779-1786, 2014.
81. Li CY, Deng W, Liao XQ, Deng J, Zhang YK and Wang DX: The effects and mechanism of ginsenoside Rg1 on myocardial remodeling in an animal model of chronic thromboembolic pulmonary hypertension. Eur J Med Res 18: 16, 2013.